IJIE

INTERNATIONAL JOURNAL OF INTEGRATED ENGINEERING
ISSN: 2229-838X e-ISSN: 2600-7916

Vol. 18 No. 2 (2026) 141-154
https://publisher.uthm.edu.my/ojs/index.php/ijie

Computational Analysis of Hyperthermia Therapy on Breast Tumors

Nur Amani Hanis Roseman[1], Mohamad Saddam Kamarudin[1], Ishkrizat Taib[1]*, Ahmad Mubarak Tajul Arifin[1], Abdul Rahman Abd Majid[1], Aslam Khan Abdul Azim Khan[1], Takahisa Yamamoto[2], Mohd Nizam Mazlan[3], Awaludin Martin[4]

[1] *Department of Mechanical Engineering, Faculty of Mechanical Engineering and Manufacturing, Universiti Tun Hussein Onn Malaysia, Batu Pahat, Johor, 86400, MALAYSIA*
[2] *Department of Mechanical and manufacturing Engineering, National Institute of Technology, Gifu College, 2236-6 Kamimakuwa, Motosu, Gifu 501-0461, JAPAN*
[3] *Aras Biomed Resources Sdn Bhd, No 22A, Jalan Kedidi, P9G/6, Presint 9, Putrajaya, MALAYSIA*
[4] *Mechanical Engineering Department, Univertas Riau, Pekanbaru 28293, INDONESIA*

*Corresponding Author: iszat@uthm.edu.my
DOI: https://doi.org/10.30880/ijie.2026.18.02.012

Article Info

Received: 15 November 2025
Accepted: 20 March 2026
Available online: 28 April 2026

Keywords

Hyperthermia therapy, tumor geometry, heat propagation, computational fluid dynamic (CFD)

Abstract

Hyperthermia therapy is a beneficial complementary approach in cancer management, facilitating the elevation of tumor tissue temperature to optimize the efficacy of chemotherapy or radiotherapy. The research aims to investigate the influence of tumor volume and quantity on its thermal behavior during hyperthermia, using Computational Fluid Dynamics (CFD) simulation. Simplified spherical breasts and tumors models were utilized to isolate the effects of tumor size and configuration. It encompassed of both single and triple tumors with diameters of 2 cm and 4 cm. The CFD simulation employed ANSYS Fluent and incorporated governing equations including continuity, Navier-Stokes, energy and Pennes bioheat equation to model fluid and heat transfer through biological tissue. The findings show that tumor size significantly affects thermal behavior during hyperthermia. Smaller tumors (2 cm) reach peak temperature of 48-58 °C with an average heating rates of 3.45 to 5.39 °C/cm and the steepest gradients is up to 16.15 °C/cm. This exhibit a more consistent and higher temperature across the tumor volume due to rapid heating and lower thermal mass. In contrast, larger tumor (4 cm) achieve a slightly higher peak temperature of 49-59°C but with a slower average heating rates of 2.14 to 2.42 °C/cm. These large tumors developed a much wider and persistent high temperatures regions but with a slower temperature decay toward surrounding healthy breast tissues which indicates greater heat retention and thermal inertia. In the configuration of triple 2 cm tumors, the thermal zones overlapped at higher surface temperatures whereas the triple 4 cm tumors produce largely separated thermal regions. These demonstrate that the large tumors

volume lead to a reduction in heat overlap and an uneven thermal fields. Overall, the results demonstrated that both tumor size and configuration significantly influence heat distribution. The CFD modelling proved to be a dependable, non-invasive technique to improve hyperthermia treatment planning for even heating and precise tumor targeting.

1. Introduction

Hyperthermia therapy has emerged as an effective adjunctive approach in cancer treatment as it targets tumors while sparing surrounding normal tissues [1], [2]. This therapeutic modality functions by raising the temperature within cancerous tissues to a range of 40 °C to 45 °C, thereby inducing cellular damage and enhancing the efficacy of conventional cancer treatment such as radiotherapy and chemotherapy [3]-[5]. Tumor characteristics specifically the tumor quantity and volume can influence thermal distribution during localized hyperthermia heating as its impact on the thermal gradients, heat retention as well as the uniformity of heat distribution [12]. Understanding these associations is crucial to optimize hyperthermia treatment protocol which tailored to specific tumor presentations.

Breast cancer has remained as one of the most prevalent malignancies worldwide [6]. The breast tissues are structurally complex as they're comprised of layered regions of skin, adipose tissue, glandular lobules and stromal components which include connective fibers, fibroblast, extracellular matrix and vascular structure [7]. These elements provide mechanical supports that modulate tissue perfusion which influence heat propagation during localized hyperthermia intervention. Breast tumors can develop at varying depth within these tissue layers from a small, confined tumor under 2 cm in size to an intermediate tumor that can range between 2 to 5 cm and large tumor lesion may even progress up to 5 cm in size [8]. These substantially alter the thermal conduction pathways and the sensitivity toward cancer treatments.

Breast tumors are characterized by abnormal vasculature, increased interstitial fluid pressures and regions of hypoxia due to rapid growth and metabolism [9]. These unique microenvironments reduce oxygen diffusion and develop surroundings that are inherently resistant to certain radiotherapy and chemotherapy treatments. These hypoxic regions in tumors are usually accompanied by an acidic extracellular pH resulted from glycolytic metabolism as well as poor perfusion. The therapeutic window of 40 to 45°C in hyperthermia therapy is needed as temperature below 40 °C fails to induce cytotoxicity in this resistant microenvironment whereas an exceeding temperature of 45 °C may risk damaging surrounding healthy vasculature and tissue structure. Hyperthermia selectively sensitizes hypoxic and acidic tumor cells when apply within this optimized range by inhibiting DNA repair mechanism, denaturing certain protein and disrupting membrane integrity [10]. Hyperthermia has also shown to induce vasodilation which led to an improvement in oxygen availability, thereby rendering tumors cells more susceptible and augmenting the cytotoxic effect to other therapies [3], [5]. These physiological effects are advantageous in breast cancer lesion treatment as hypoperfusion, and thermal heterogeneity impede the usual conventional therapies.

One of the major challenges in the application of hyperthermia for breast tumor is in achieving controlled and uniform heating across the tumor of different size and configurations. The breast tissue glandular to fat composition may vary between individuals as well as the different quadrant of the same breast which may affect the thermal conductivity and the heat retention [11]. Besides, the presence of blood vessels that either traverse or lie adjacent to the breast tumor mass might act as a critical heat sink in that way, altering the thermal gradient [12]. Blood perfusion serves as the main mechanism in heat dissipation in living tissues [13]. This creates a dynamic balance between energy deposition from hyperthermia and the convective cooling from the circulating blood. The perfusion mediated heat transfer is mathematically described by the Pennes-Bioheat equation which models the tissue temperature distribution by integrating the metabolic heat generation [14]. The variations in perfusion rate may alter the depth of heat penetration achieved during hyperthermia therapy particularly in breast tissue where adipose and glandular regions show different vascular densities [14], [15]. The structural and physiological complexities pinpoint the significance of precise characterization of thermal behavior within breast tissue to guarantee a safe and effective hyperthermia delivery.

Recent advancements in computational approaches have significantly enhanced the effectiveness and accuracy of hyperthermia therapy. Computational fluid dynamics (CFD) simulations are increasingly employed to model heat distributions within biological tissues, offering predictive assessment of temperature profiles in tumors throughout of hyperthermia treatments [14]-[16]. These simulations can act as a guide for treatment planning by optimizing factors such as the power delivered, the configuration used, and the duration of the treatment, thereby improving patient outcomes [16].

Previous studies demonstrate that numerical simulations are vital for understanding the thermodynamic behavior of tumor tissues, which can be crucial for tailoring hyperthermia strategies that will yield the most heat in cancers while leaving surrounding normal tissues minimally affected [17], [18]. The use of novel materials such

Int. Journal of Integrated Engineering Vol. 18 No. 2 (2026) p. 141-154

as magnetic nanoparticles has enabled localized hyperthermia that results in more focused heating and better therapeutic consequences [19], [20]. Building off the basic principles above, the researcher may improve techniques for applying hyperthermia to reduce side effects for normal cells, making a stronger case for hyperthermia a key in multi domain treatment for cancer [21], [22]. The potential of hyperthermia is also enhanced by its use with immunotherapy, which allows for enhanced use of the body's own immune processes to treat cancer [5], [21].

The integration of hyperthermia, computational modeling, and new materials potentially provides a promising opportunity for cancer treatment [14]. Continued research aimed at elucidating the mechanisms underlying hyperthermia and their relationships with other treatment modalities, is likely to alter future treatment strategies in oncology, thus enhancing outcomes for cancer patients. Building in this foundation, this study focuses on the geometry of tumors, their sizes and number as well as how it affects the heat propagation during the hyperthermia procedure. By simulating varying tumors diameter, this research aims to improve the understanding of thermal behavior of tumor tissues under a controlled heating setting. Notably, the findings of this study convey direct relevance to clinical practice and thermal device designing, since accurate prediction of temperature distribution is vital for defining the safe input power, adjustment heat applicator placement and confirming total thermal coverage of the tumor areas. The present study therefore provides computational understanding as well as the refinement of patient-specific hyperthermia therapy planning and the development of more effective hyperthermia delivery systems.

2. Methodology

2.1 Simplified Geometry of Tumors

3D geometries models were generated in ANSYS software for this simulation study using Design Modeler. Two types of geometry represent different breast tumor representations were created. A simplified spherical of 14 cm in diameter breast model with 3 mm blood vessel was developed to better yield a stable simulation and focus more on the influence of heat on tumor sizes. Next, single and triple tumors models with diameters of 2 cm and 4 cm were chosen based on the clinically reported size ranges commonly utilized in breast cancer classification systems, as shown in Figs. 1 and 2. According to Cancer Research UK staging criteria, breast tumors are classified as T1 lesions with the measurement of ≤2 cm while tumors measuring to > 2 cm and ≤ 5 cm fall under the T2 category [8], [23]. The sizes group used in this study represent average presentation in the early to mid-stage of breast cancer. The selection of 2 cm and 4 cm tumor diameters allowed sufficient acquiring of thermal behavior that is therapeutically relevant and clinically prevalent to this study. These two sizes enable good comparison of heat propagation between small and moderately large tumors. Besides, the configurations of single and triple tumors were designed to simulate the solitary and clustering effect that arises in some cancer cases. These geometries aid to determine the influence of tumor size and number of tumors on heat distribution during hyperthermia.

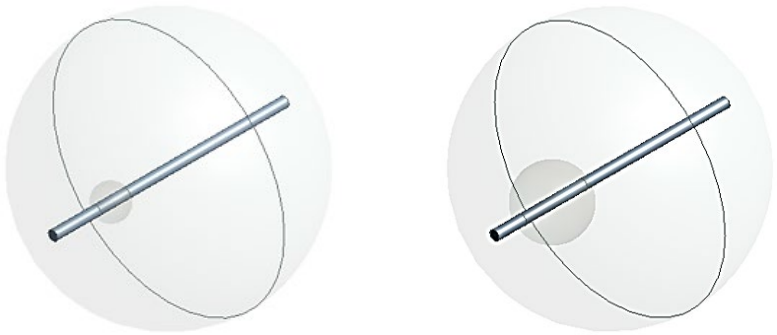

(a) **(b)**

Fig. 1 *The geometry of a single tumor with diameter (a) 2 cm; (b) 4 cm*

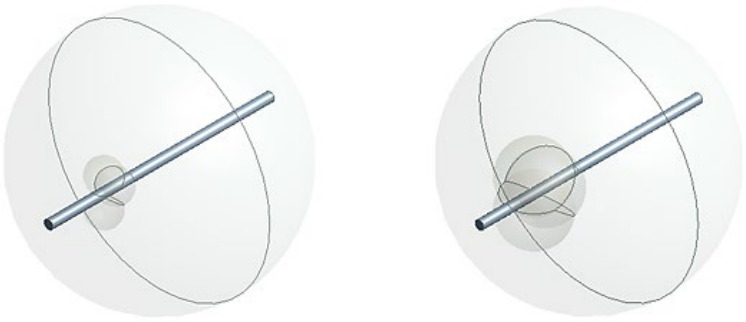

(a) (b)

Fig. 2 *The geometry of triple tumors with diameter (a) 2 cm; (b) 4 cm*

2.2 Discretization Technique

Tetrahedral element meshing of the tumor geometries was utilized to best reflect the natural feature of the geometry for biological tissues [14], [24], [25]. An element size of 0.0002 mm was used to develop high-resolution mesh around the feature of interest the tumor structure and in the tissue region as this region is expected to exhibit steep temperature gradients and noteworthy heat transfer interaction during hyperthermia treatment (Table 1). A clear visual of tetrahedral mesh generated is shown in Fig. 3. The Grid independence test (GIT) was performed to check the mesh resolution [26]. Percentage error (Eq. 1) was calculated to determine the mesh quality and refinement. A finer mesh generally provides a better representation of the temperature gradients or heat propagation and is especially critical around the tumor boundary region.

This provides the assurance that the simulation will truly demonstrate the physical model and not merely a numerical coincidental. By confirming the mesh independence, the simulation outputs could be relied upon to assess performance of hyperthermia treatment approaches.

$$\text{Percentage error} = \left|\frac{T_{2cm} - T_{4cm}}{T_{4cm}}\right| X\ 100 \tag{1}$$

where T_{2cm} is temperature value for 2cm tumor whereas T_{4cm} is temperature for 4cm tumor.

Table 1 *Meshing of breast models*

Geometry	One tumor		Three tumors	
	2 cm	4 cm	2 cm	4 cm
Number of Nodes	303464	139772	351719	341435

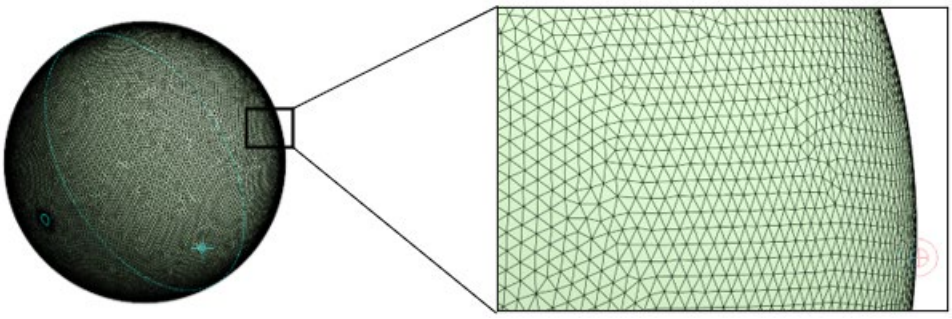

Fig. 3 *Tetrahedral meshing*

2.3 Governing Equations

To model computational heat transfer and fluid flow processes in biological tissues, focusing on tissues with tumors, several mathematical equations are employed to capture the complexity of fluid flow and heat transfer. The equations are used to maintain mass conservation, track the motion of the fluid, and determine heat transfer

Int. Journal of Integrated Engineering Vol. 18 No. 2 (2026) p. 141-154

[14]. The continuity equation (Eq. 2) maintains mass conservation on a variety of levels. The amount of fluid entering a volumetric region equals the amount of fluid leaving a volumetric region, hence no mass is created or destroyed. Thus, blood that flows into the tissue must also flow out of the system or must remain unchanged in the system.

$$\nabla . V = 0 \tag{2}$$

where v is the fluid velocity, and the velocity components in each direction sum to zero, thus no fluid is lost or created.

The Navier-Stokes equation (Eq. 3) describes fluid motion. It looks upon the forces acting on fluids, pressure on the fluid, viscosity, and body forces. This equation allowed the simulation of fluid movement and applied to investigate the influence of internal forces and external conditions to fluid motion.

$$\rho \frac{dV}{dt} = -\nabla_p + \nabla . \tau + \rho f \tag{3}$$

Where ρ is the fluid density, V is the velocity, p is the pressure, τ represents viscous forces, and f represents any external forces. This equation is used to simulate blood flow through the tissues, considering the forces that promote or create resistance to blood flow. The Energy equation (Eq. 4) governs the distribution of heat in the system by considering the conduction fluid movement, and heat produced by biological processes within the body.

$$\rho \left(\frac{\partial h}{\partial t} + \nabla . (hv) \right) = \frac{dp}{dt} + \nabla . (k \nabla \mathrm{T}) + \varphi \tag{4}$$

where h is the specific enthalpy, T is the temperature, k is the thermal conductivity (how easily heat spreads) and ϕ represents any additional heat generation due to fluid movement or other factors.

The specific enthalpy, h, is related to temperature through $h=C_pT$, assuming constant specific heat capacity. This relationship allows the energy equation to be reformulated in terms of temperature which ensures consistency with Pennes-Bioheat equation (Eq. 5) that describes the heat transfer in biological tissues using temperatures as the main variable and includes the blood flow as well as metabolic heat production from the cells. In the tissues, blood serves as a carrier of heat, and its flow rate influences the distribution of the heat. Heat generated within the cells from metabolic processes is also considered. This equation is expected to model or simulate heat transfer processes occurring in tissues.

$$\rho_t C_t \left(\frac{\partial T_t}{\partial t} \right) = \nabla . (k_t \nabla T_t) + \rho_b C_b \omega_b (T_a - T_i) + Q_{met} \tag{5}$$

where T_t is the tissue temperature, $\rho_t, C_t \; and \; k_t$ are the tissue's density, specific heat, and thermal conductivity, $\rho_b C_b \; and \; \omega_b$ are the blood's density, specific heat, and perfusion rate (blood flow) T_a is the arterial blood temperature and Q_{met} is metabolic heat generation. These equations collectively capture the conduction, metabolic heat generation and the perfusion induced convection in the breast tissue.

2.4 Parameter Assumptions

Several thermal and physical characteristics were assumed based upon previous literature values for the measurement of specific biological properties during simulation studies [14], [27]. In this study, the tissue density was assumed to be 1200 (kg/m^3) which falls within typical density range for biological soft tissue in computational thermal simulations. The blood density was taken as 1060 (kg/m^3). The specific heat capacities were taken as 1050 (J/kg·K) for tissue, 3950 (J/kg·K) for blood, and the tumor tissue was assigned a specific heat capacity of 3660 J/kg·K. The thermal conductivity values were taken as 3500 (J/kg·K) for tissue, 0.37 (W/m·K) for blood, and 0.52 (W/m·K) for tumor tissue as shown in Table 2. Each of these values are appropriate in defining how heat may be conducted, stored, and dissipated through biological media.

Table 2 *Parameter assumptions of hyperthermia therapy [14]*

Parameter	Value
Tissue density, ρ	1200 (kg/m^3)
Blood density, ρb	1060 (kg/m^3)
Specific heat of tissue, C	1050 (kg/m^3)
Specific heat of blood Cb	3950 (J/kg. K)
Specific heat of tumor, Ct	3660 (J/kg. K)
Thermal conductivity of tissue k	3500 (J/kg. K)
Thermal conductivity of blood kb	0.37 ($W/m.K$)
Thermal conductivity of tumor, kt	0.52 ($W/m.K$)

3. Results and Discussion

3.1 Grid Independence Test

A grid independence test was performed to confirm that the simulations were not affected by the mesh density. This step is important in computational fluid dynamics as it shows the solution is stable and independent of the grid size. Several mesh densities were made of both tumors, and a comparison of the resulting temperatures was made to gauge the model's sensitivity to mesh density.

As presented in Fig. 4, the chart demonstrated that there was very little variation in temperature results with each level of mesh density. The values plotted generally indicated a trend that began to stabilize, even further reducing the mesh size. In Table 3, the comparison between temperature at 2 cm and 4 cm showed a minor discrepancy with the highest percentage error at 2.56%. The average error across all measurements was approximately 0.76%, thus demonstrating strong consistency of temperature profiles between 2 cm and 4 cm. Percentage errors less than 5% imply that the simulation setup used is reliable with only negligible deviations and further mesh refinement would not significantly alter the numerical solution. This behavior demonstrates grid independence was achieved and the density of mesh selected was adequately dense enough to capture thermal behavior in biological tissues during hyperthermia as well as maintaining reasonable computational time and cost.

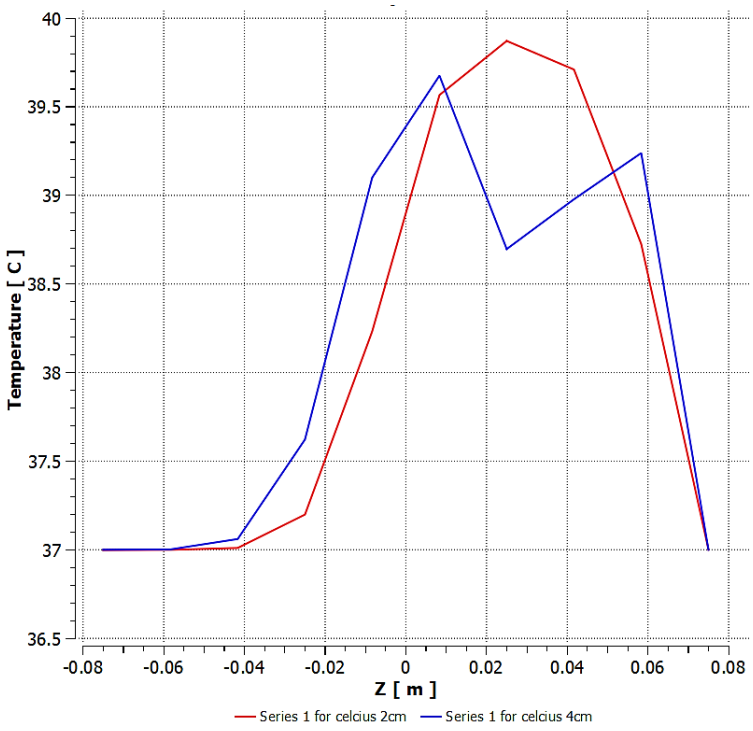

Fig. 4 *Graph of GIT*

Int. Journal of Integrated Engineering Vol. 18 No. 2 (2026) p. 141-154

Table 3 *Percentage error in grid independence test*

Temperature, 4 cm (°C)	Temperature, 2 cm (°C)	Absolute difference	Percentage error (%)
36.9936	36.9936	0	0
37.0036	36.9986	0.0050	0.0135
37.0634	37.0036	0.0598	0.1617
37.6268	37.1980	0.4288	1.1528
39.0976	39.5613	0.4637	1.1720
39.6759	39.8704	0.1944	0.4877
38.6937	39.7108	1.0171	2.5613
39.2372	38.7336	0.5036	1.3003
36.9986	36.9986	0	0

3.2 Heat Propagation of Single Tumor

Figs. 5 to 7 illustrates the temperature within the breast models subjected to different surface heating conditions of 40, 45 and 50 °C, respectively. At 40 °C, the temperature elevation was primarily confined to the tumor region which indicates efficient localized heating. The 2 cm tumor demonstrated a well-defined thermal region with maximum temperatures ranging between 46 °C to 48 °C. In contrast, the 4 cm tumor shows a much broader heat distribution with a slightly higher central temperature of approximately between 48 °C to 49 °C. This pattern implies that a larger tumor retained more heat during hyperthermia due to its lower surface-area-to-volume ratio.

With the increased heating temperature to 45 °C, both tumor models demonstrated an expanded high temperature area. The 4 cm tumor showed a more gradual temperature gradient, indicating a higher degree of internal heat accumulation. At 50 °C initial hyperthermia temperature, the temperature distribution across the 2 cm tumor became nearly uniform and reaches as high as 55 °C. In addition, the 4 cm tumor exhibited a more definite thermal gradient with the central region exceeding 57 °C and maintaining around 45 °C to 48 °C at the periphery. These findings confirm that the tumor size has significant influence on the internal heat propagation and thermal retention of tumor tissue during hyperthermia therapy.

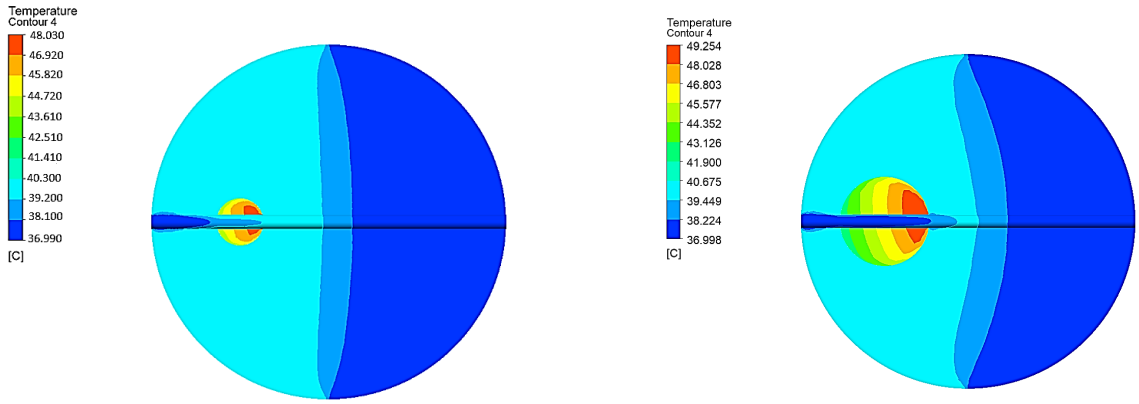

(a) **(b)**

Fig. 5 *Heat propagation 40 °C single tumor (a) 2 cm tumor; (b) 4 cm tumor*

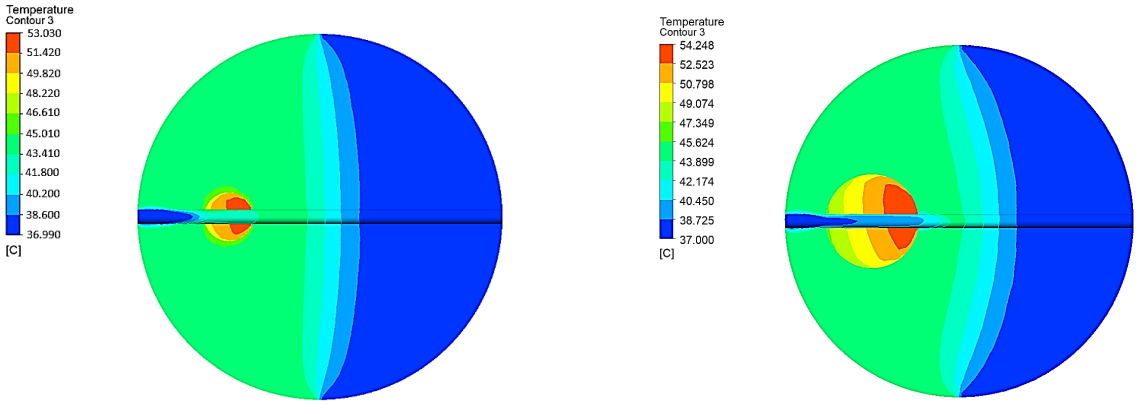

Fig. 6 *Heat propagation 45 °C single tumor (a) 2 cm tumor; (b) 4 cm tumor*

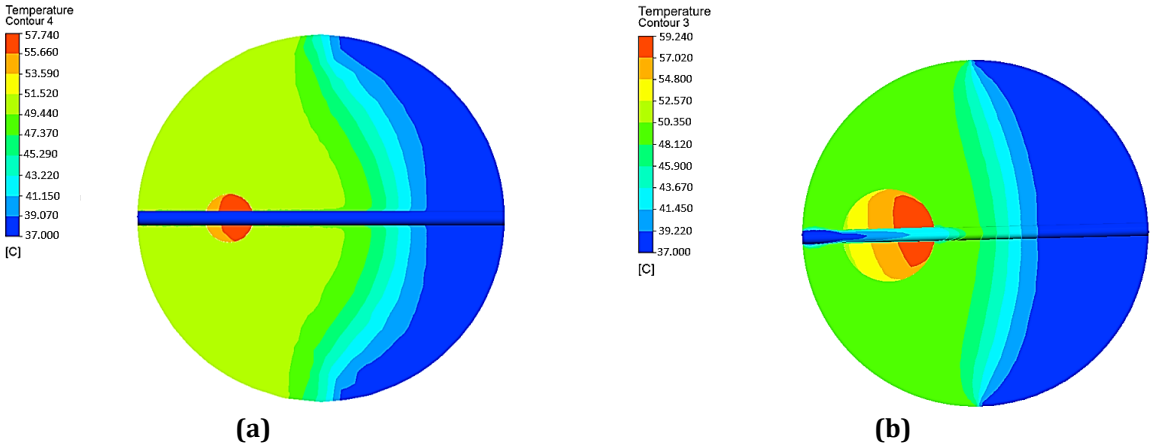

Fig. 7 *Heat propagation 50 °C single tumor (a) 2 cm tumor; (b) 4 cm tumor*

In addition, Figs. 8 and 9 presented the temperature profiles that were extracted along the central axis passing through the tumor for further observation of heat distribution. In both cases of 2 and 4 cm tumors, the temperature peaked within the tumor core and decreased gradually as it reaches normal breast tissue region. The 2 cm tumor in Fig. 8 exhibited a sharp temperature gradient at the tumor boundary which suggests that a confined heating zone as well as a rapid dissipation into adjacent breast tissue. On the contrary, the 4 cm tumor in Fig. 9 displayed a much broader plateau region at the elevated temperature, indicating slower cooling, lower heat dissipation and enhanced heat retention within the tumor core. The differences in core temperature between 2 and 4 cm is due to the thermal resistance within the tumor volume. As the distance between the hyperthermia heat source and the tumor core increases, the internal thermal resistance also increases while the rate of heat conduction reaching the center of tumor will then be reduced, thus resulting in less thermal energy accumulation at the core region.

The difference in the heat distribution behavior between the two tumor sizes can be attributed to the variations in geometric and physiological characteristics of the tumors themselves. Larger tumors have a much lower surface area to volume ratio and commonly exhibit a poorer vascular perfusion which results in a decrease in convective heat loss as well as a longer thermal relaxation time. Contrary to that, smaller tumors experience faster heat transfer to surrounding breast tissue but express a limitation in the duration of effective therapeutic heating. These results align with previously reported study by Mahmoud et al. [28] on hyperthermia heat transfer in biological tissue where the findings showed that a lower perfusion and a higher density in malignant tissue regions promote greater heat accumulation.

These findings demonstrate that tumor tissue absorbs and retain heat more effectively than healthy normal breast tissue. The degree of heat retention is influenced by the tumor size and structure. This characteristic proves that larger tumor sizes retain heat more effectively compared to smaller tumors but require longer heating duration or higher power to achieve uniform thermal coverage. The utilization in the inherent physical differences

Int. Journal of Integrated Engineering Vol. 18 No. 2 (2026) p. 141-154

of heat absorption between the breast tumor and healthy tissue enables a more effective and targeted hyperthermia therapy procedure.

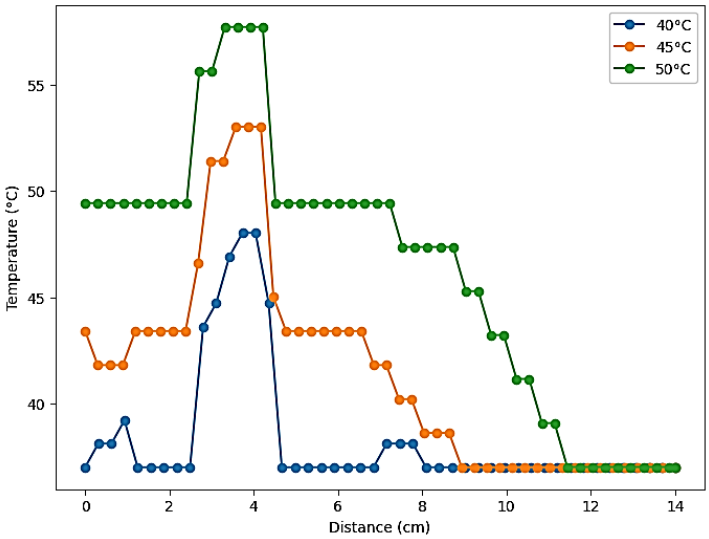

Fig. 8 *Temperature distribution along central axis through 2 cm single tumor*

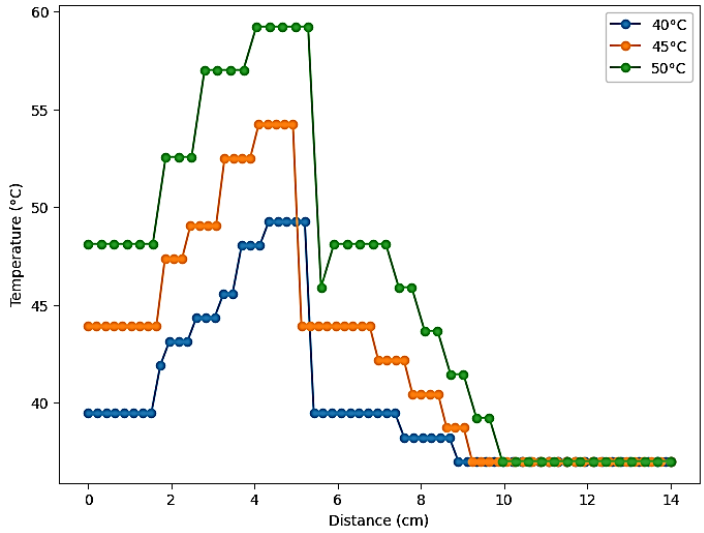

Fig. 9 *Temperature distribution along central axis through 4 cm single tumor*

3.3 Heat Propagation of Triple Tumor

Figs. 10 to 12 displays the thermal behavior of the triple tumor configurations which are affected by the extend of heating as well as the degree of thermal interaction between adjacent tumors during hyperthermia session. The 2 cm triple tumors exhibited a rapid elevation of temperature and early formation of thermal regions. At 40 °C, each tumor reached a localized high temperature region ranging from approximately 43 °C to 47 °C as the heat penetrated quickly through the small tumor mass and progressed laterally toward neighboring tumor tissues. The thermal contours overlap which indicates the onset of thermal coupling within the tumor cluster. This effect became more pronounced at 45 °C where the heating generated a continuous band of increased temperature fully connecting all three tumors. The central region reached a temperature that exceeded 52 °C thus forming a fused area of therapy rather than separate temperature peaks. Besides, the high temperature core intensified further at 50 °C reaching up to 56 to 58 °C which occupies a large central tumor area. These results demonstrate that small and closely spaced tumors tend to behave collectively under hyperthermia therapy. The heat conduction produces merged thermal fields that encompassed the entire tumor cluster.

On the contrary, the 4 cm triple tumors exhibited a distinctly thermal behavior due to larger volume and advanced thermal mass. At 40 °C, each tumor developed a wider but visibly separated heat distribution with the

central tumor temperature reaching around 46 to 48 °C. The heated tumor regions did not merge as each tumor asserted a recognizable thermal boundary. At 45 °C hyperthermia heating, the heated area around each tumor becomes broader and the thermal fields remain mainly independent with the cores reached up to 52 to 54 °C. Moreover, the cores of the triple 4 cm tumors reach the highest temperature at 58 to 60°C when heated at 50 °C, demonstrating a strong internal heating. Nevertheless, the degree of heat merging remained limited in comparison to 2 cm tumors cluster even with such an elevated temperature. Consequently, the thermal inertia which is the resistance to temperature change is greater with larger tumor size. The findings highlighted slow heat spread and heat dissipation that restricts overlapping of heat conduction thereby, limiting uniformity and efficiency of thermal distribution.

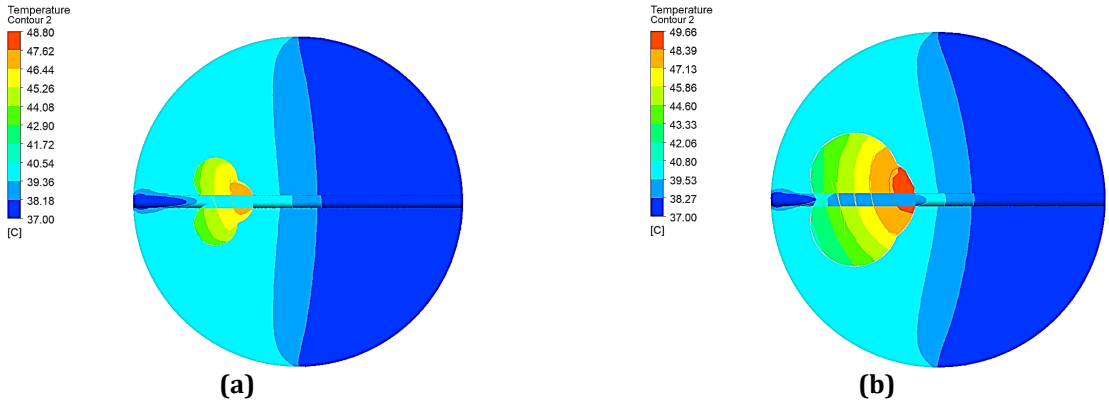

Fig. 10 *Heat propagation 40 °C triple tumors (a) 2 cm tumor; (b) 4 cm tumor*

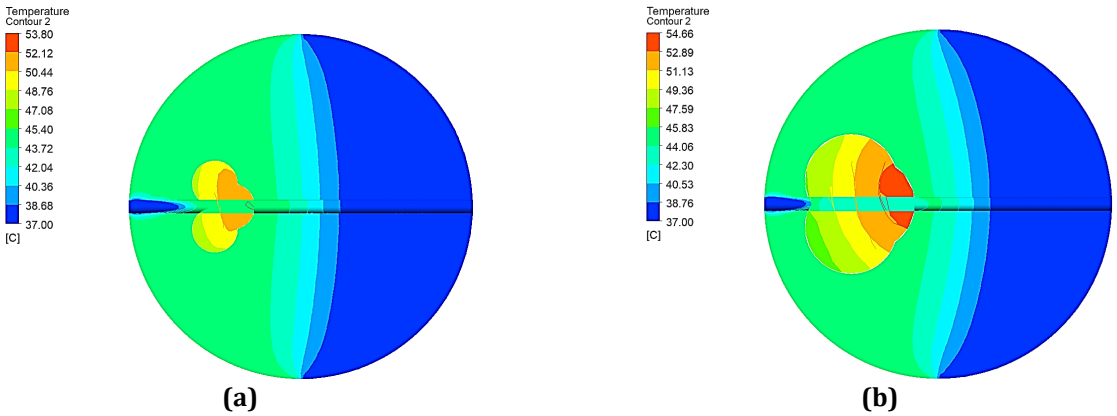

Fig. 11 *Heat propagation 45 °C triple tumors (a) 2 cm tumor; (b) 4 cm tumor*

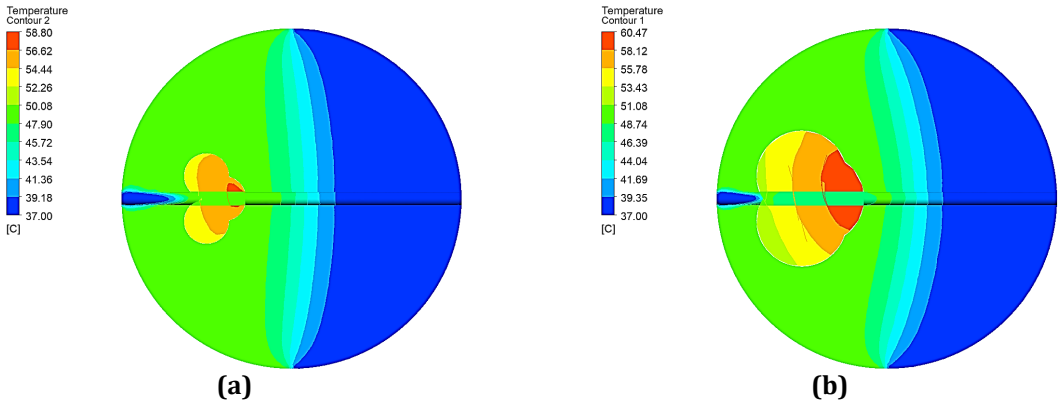

Fig. 12 *Heat propagation 50 °C triple tumors (a) 2 cm tumor; (b) 4 cm tumor*

Int. Journal of Integrated Engineering Vol. 18 No. 2 (2026) p. 141-154

In Fig. 13, the temperature profile across the triple tumors forms a single broad peak which confirms the merging of thermal zone. At 40 °C hyperthermia heating, the temperature increases from the baseline to a peak of about 47 to 48 °C with a slight dip of only 1.2 °C between tumors, indicating initial stage of the thermal merging with approximately 85% thermal zone overlapping. Besides, the merged area becomes flatter and wider during the 45 °C heating with inter-tumor temperature variation reducing to less than 0.5 °C, which suggests that all three tumors reach uniform heating level corresponding to more than 95% thermal filed merging. At 50 °C heating, the peak temperature exceeds 57 °C with higher temperature plateau maintained across a continuous region spanning 3.2 cm demonstrating deep heat penetration. These demonstrate a deep heat penetration resulting in a larger uniform heat region across the tumor cluster. Hence, a smaller tumor cluster acts thermally as a single entity once hyperthermia heating is applied. Low thermal inertia and their small volume aloe rapid heat transfer thus, merging the temperature field of neighboring tumors. However, with significant thermal synergy reach even in moderate hyperthermia heating, the risk of overheating surrounding healthy tissues also increases.

Fig. 14 displays the temperature distribution of triple 4 cm tumors. Each tumor cluster forms three distinct temperature peaks. At 40 °C, the temperature elevated to approximately 48 to 50 °C, yet the dip between peaks stays low (~44°C) representing a 4 to 6 °C temperature differential, implying limited heat coalescence with only 30 to 40% thermal zone overlap. This can also be observed at 45 °C and 50 °C hyperthermia heating with result showing broader peak widths but discrete temperature cores. The inter-tumor temperature differences persist at 3 to 5°C even at the highest temperature setting. The line profile shows lower thermal synergy between tumors with only thermal overlap of 45 to 55% at 45 °C and 60 to 65% at 50 °C since larger tumors heat slower with minimal heat interaction.

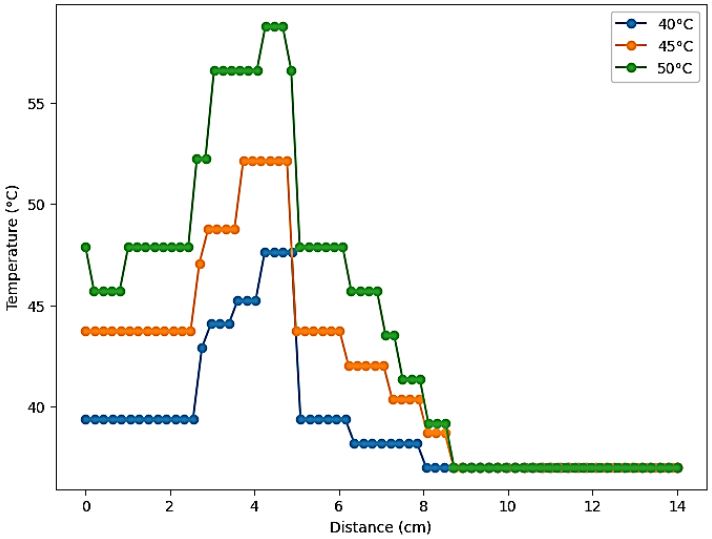

Fig. 13 *Temperature distribution along central axis through 2 cm triple tumors*

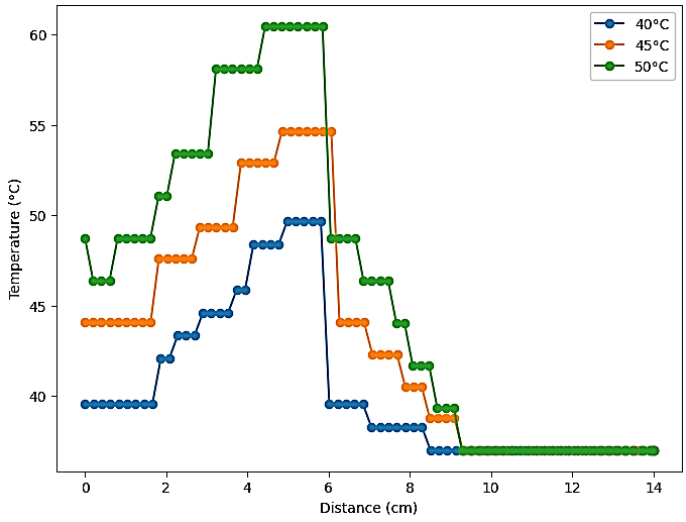

Fig. 14 *Temperature distribution along central axis through 4 cm triple tumors*

4. Conclusions

The study demonstrates that breast tumor size and spatial configuration exert a substantial influence on the heat distribution during hyperthermia therapy. Smaller tumors exhibited rapid heating and strong thermal interaction while clustered with temperature differentials between single and triple configurations of 2 to 3 °C at peak heating and thermal overlap raising from isolated hotspots to more than 95% coalescence in the 2 cm triple tumor configuration. In contrast, larger tumors showed wider high temperature regions but separate thermal areas when tumors were clumped together with inter-tumor temperature differential persisting at 3 to 5 °C even during the highest clinical temperature setting. The thermal overlap does not exceed 65% in the 4 cm triple tumor configuration. Further observation revealed that the most efficient hyperthermia temperature varies depending on the tumor size. For both 2 cm single and triple tumor configurations, 45 °C provided the most balance between heating and controlled thermal spread which achieved peak temperatures of 52 to 54 °C with minimal overrun beyond target temperature margins. On the other hand, 50 °C showed the most optimal temperature input for 4 cm tumor to achieve unform heating as lower temperatures were deemed insufficient to overcome their thermal inertia. At 40 °C and 45 °C temperature settings, the temperature differentials range between 4 to 6 °C in the tumors cores thus confirming the inadequate thermal penetration.

This study highlights the requirement to incorporate tumors size and configuration when planning hyperthermia therapy to ensure consistent thermal coverage and reducing overheating to surrounding healthy breast tissues. Tailoring the hyperthermia temperature to the tumor size may improve the probability of achieving therapeutic temperature that enhances the synergistic effects for conventional tumor or cancer treatments. Integrating these insights into clinical practice will allow safer, more effective and more predictable hyperthermia planning for patients with multifocal or heterogenous breast tumors. In summary, this study demonstrates that CFD can be a non-invasive method to systematically appraise and optimize hyperthermia treatment planning. Simulating heat distribution across different tumor configurations helps reduce treatment planning time while enabling clinicians to pre-select optimal power settings and exposure duration before treatment begins. As described by the simulated realistic tumor space, integrating changes to treatment input power and tumor arrangements could contribute positively to overall treatment effectiveness and safety.

5. Recommendation for Future Work

For further investigation, it is recommended to incorporate tissue damage models such as cumulative equivalent minutes at 43 °C (CEM43) to directly relate the simulated heat propagation with predicted tissue necrosis and thermal therapeutic efficacy. Expanding the thermal simulation to include different tissue layer properties, varying perfusion rates and anisotropic heat transfer would also enhance the physiological realism in biological tissue which allow more accurate computational prediction. Additionally, adding blood vessel networks of variable diameter as well as branching patterns could help in clarifying the influence of vascular sinks on temperature consistency. Integrating experimental validation using physical breast tumor phantoms or inserting in vivo measurements is commended to reinforce the numerical findings in this study. Lastly, including an optimization study which explores multi source hyperthermia delivery or utilization of patient-specific tumor geometries derived from Magnetic Resonance Imaging (MRI) scan may further improve the development of targeted and personalized hyperthermia therapy planning.

Acknowledgement

This research was supported by the Malaysian Ministry of Higher Education (MOHE) through the Fundamental Research Grant Scheme (FRGS) (FRGS/1/2022/TK10/UTHM/03/5).

Conflict of Interest

Authors declare that there is no conflict of interest regarding the publication of the paper.

Author Contribution

The authors confirm contribution to the paper as follows: ***study conception and design:*** *Taib I, Arifin AMT;* ***data collection:*** *Roseman NAH, Majid ARA, Khan AKAA;* ***analysis and interpretation of results:*** *Roseman NAH, Majid ARA, Khan AKAA;* ***draft manuscript preparation:*** *Roseman NAH, Kamarudin MS, Majid ARA, Khan AKAA. All authors reviewed the results and approved the final version of the manuscript.*

References

[1] David M. Smadja (2024) Hyperthermia for targeting cancer and cancer stem cells: insights from novel cellular and clinical approaches, Stem Cell Reviews and Reports, 20(6), 1532-1539, https://doi.org/10.1007/s12015-024-10736-0

[2] Tine Logghe, Eke van Zwol, Benoit Immordino, Kris Van den Cruys, Marc Peeters, Elisa Giovannetti & Johannes Bogers (2024) Hyperthermia in combination with emerging targeted and immunotherapies as a new approach in cancer treatment, Cancers, 16(3), 505, https://doi.org/10.3390/cancers16030505

[3] Fatih Goksel & Fatih Demircioglu (2020) Evaluation of Oncological Hyperthermia Centers and Turkey Modeling Oncological Hyperthermia Centers and Turkey Modeling, Research Square, 1-10, https://doi.org/10.21203/rs.3.rs-27512/v1

[4] Johannes Crezee, Nicolaas AP Franken & Arlene L. Oei (2021) Hyperthermia-based anti-cancer treatments, Cancers, 13(6), 1240, https://doi.org/10.3390/cancers13061240

[5] David Chang, May Lim, Jeroen ACM Goos, Ruirui Qiao, Yun Yee Ng, Friederike M. Mansfeld, Michael Jackson, Thomas P. Davis & Maria Kavallaris (2018) Biologically targeted magnetic hyperthermia: Potential and limitations, Frontiers in Pharmacology, 9, 831, https://doi.org/10.3389/fphar.2018.00831

[6] Melina Arnold, Eileen Morgan, Harriet Rumgay, Allini Mafra, Deependra Singh, Mathieu Laversanne, Jerome Vignat, Julie R. Gralow, Fatima Cardoso, Sabine Siesling & Isabelle Soerjomataram (2022) Current and future burden of breast cancer: Global statistics for 2020 and 2040 The Breast, 66, 15-23, https://doi.org/10.1016/j.breast.2022.08.010

[7] Swarajit Kumar Biswas Saswati Banerjee, Ginger Wendolyn Baker, Chieh-Yin Kuo & Indrajit Chowdhury (2022) The mammary gland: basic structure and molecular signaling during development, International Journal of Molecular Sciences, 23(7), 3883, https://doi.org/10.3390/ijms23073883

[8] Cancer Research UK (2023, May 17). TNM staging for breast cancer. https://www.cancerresearchuk.org/about-cancer/breast-cancer/stages-grades/tnm-staging

[9] Ebbe Boedtkjer & Stine F. Pedersen (2020) The acidic tumor microenvironment as a driver of cancer, Annual Review of Physiology, 82(1), 103-126, https://doi.org/10.1146/annurev-physiol-021119-034627

[10] Ivana Gorbaslieva, Tom Quisenaerts, Johannes JPM Bogers, Marc Peeters, Vera Saldien & Dirk Ysebaert (2025) Temperature-dependent effects of induced hyperthermia, including whole-body hyperthermia, on the hallmarks of cancer: A systematic review, Cancers, 17(23), 3824, https://doi.org/10.3390/cancers17233824

[11] Jeantide Said Camilleri, Lourdes Farrugia, Sergio Curto, Dario B. Rodrigues, Laura Farina, Gordon Caruana Dingli, Julian Bonello, Iman Farhat & Charles V (2022). Review of thermal and physiological properties of human breast tissue. Sensors, 22(10), 3894, https://doi.org/10.3390/s22103894

[12] Manpreet Singh (2022) Blood perfusion extraction in cancerous lesions using thermal signatures of infrared imaging, Inverse Heat Transfer and Anisotropic Voxel Based Mapping of MicroCT Imaging: Modelling and Simulation, http://doi.org/10.2139/ssrn.4029435

[13] Leonardo Bianchi, Fabiana Cavarzan, Lucia Ciampitti, Matteo Cremonesi, Francesca Grilli & Paola Saccomandi. (2022) Thermophysical and mechanical properties of biological tissues as a function of temperature: a systematic literature review, International Journal of Hyperthermia, 39(1), 297-340, https://doi.org/10.1080/02656736.2022.2028908

[14] Nur Maizaratul Hanisha Khairi Azhar, Ishkrizat Taib, Awaludin Martin, Ahmad Mubarak Tajul Arifin, Mohamad Saddam Kamarudin & Amani Hanis Roseman (2024) Heat propagation in multiple malignant tumours using the hyperthermia therapy, Journal of Advanced Research, 26(1), 1-21, https://doi.org/10.37934/arnht.26.1.121

[15] J. W. Hand & Gail ter Haar (1981) Heating techniques in hyperthermia, The British Journal of Radiology, 54(642), 443-466, https://doi.org/10.1259/0007-1285-54-642-443

[16] Bibin Prasad, Jung Kyung Kim & Suzy Kim (2019) Role of simulations in the treatment planning of radiofrequency hyperthermia therapy in clinics, Journal of Oncology, 2019(1), 9685476, https://doi.org/10.1155/2019/9685476

[17] Chae Ryeong Ahn, Jinbong Park, Jai-Eun Kim, Kwang Seok Ahn, Young Woo Kim, Minjeong Jeong, Hong Jun Kim, Sun Hyang Park & Seung Ho Baek (2020) Cinnamaldehyde and hyperthermia co-treatment synergistically induces ROS-mediated apoptosis in ACHN renal cell carcinoma cells, Biomedicines, 8(9), 357, https://doi.org/10.3390/biomedicines8090357

[18] N. Nizam-Uddin & Ibrahim Elshafiey. (2017) Enhanced energy localization in hyperthermia treatment based on hybrid electromagnetic and ultrasonic system: proof of concept with numerical simulations, BioMed Research International, 2017(1), 5787484, https://doi.org/10.1155/2017/5787484

[19] Mahdi Nabil & Paolo Zunino (2016) A computational study of cancer hyperthermia based on vascular magnetic nanoconstructs, Royal Society Open Science, 3(9), 160287, https://doi.org/10.1098/rsos.160287

[20] Rana M. Shehata, Mohamed I. Badawi & Nour Eldin Ismail (2021), Hyperthermia for breast cancer treatment using a slotted microstrip patch antenna array, Journal of Al-Azhar University Engineering Sector, 16(61), 1135-1155, https://doi.org/10.21608/auej.2021.207671

[21] R. F. Reis, F. S. Loureiro & M. Lobosco (2014) A parallel 2D numerical simulation of tumor cells necrosis by local hyperthermia, Journal of Physics: Conference Series, IOP Publishing, 490 (1), 012138, https://doi.org/10.1088/1742-6596/490/1/012138

[22] Yohsuke Yagawa, Keishi Tanigawa, Yasunobu Kobayashi & Masakazu Yamamoto (2017) Cancer immunity and therapy using hyperthermia with immunotherapy, radiotherapy, chemotherapy, and surgery, Journal Cancer Metastasis Treat, 3(10), 218, https://doi.org/10.20517/2394-4722.2017.35

[23] Maria L. Anzola, David Alberico, Joyce Yip, James Wiskin, Bilal Malik, Raluca Dinu, Belinda Curpen, Michael L. Oelze, and Gregory J. Czarnota (2025) Quantitative volumetric analysis using 3D ultrasound tomography for breast mass characterization, Tomography, 11(10), 111, https://doi.org/10.3390/tomography11100111

[24] Nur'Afifah Yousri, Nabilah Ibrahim, Nur Amani Hanis Roseman, Ishkrizat Taib & Shahnoor Shanta (2024) CFD based on the visualisation of aortic valve mechanism in aortic valve stenosis for risk prediction at the peak velocity, Journal of Advanced Research in Micro and Nano Engineering, 17(1), 56-68, https://doi.org/10.37934/armne.17.1.5668.

[25] Nur Amani Hanis Roseman, Muhammad Amirul Suparman, Ishkrizat Taib, Norzelawati Asmuin, Ahmad Mubarak Tajul Arifin, R. H. A. Haq, S. N. M. Mohd Yunos, Nurul Fitriah Nasir & Normayati Nordin (2019) Impact of excessive volume of cerebrospinal fluid (CSF) due to abnormality morphologies in brain and spinal cord, Journal of Advanced Research in Fluid Mechanics and Thermal Sciences, 64(2), 206-218. https://semarakilmu.com.my/journals/index.php/fluid_mechanics_thermal_sciences/article/view/3649

[26] Asral, Ridwan Abdurrahman, Wai Chang Khoo, Ishkrizat Taib, Nur Amani Hanis Roseman, Kar Hoe Kong, Cheng San Lee, Khairul Shafaiz Jesni & Awaludin Martin (2024) CFD analysis of coronavirus dispersion through breathing in aircraft cabin environments, Journal of Advances in Fluid, Heat, and Materials Engineering, 1(1), 49-59, https://doi.org/10.37934/afhme.1.1.4959a

[27] Nikhil Vaidya, Marco Baragona, Valentina Lavezzo, Ralph Maessen & Karen Veroy (2021) Simulation study of the cooling effect of blood vessels and blood coagulation in hepatic radio-frequency ablation, International Journal of Hyperthermia, 38(1), 95-104, https://doi.org/10.1080/02656736.2020.1866217

[28] Mahmoud Ragab, Ahmed E. Abouelregal, Huda F. AlShaibi & Rasha A. Mansouri (2021) Heat transfer in biological spherical tissues during hyperthermia of magnetoma, Biology, 10(12), 1259, https://doi.org/10.3390/biology10121259